Diamond & Related Materials 88 (2018) 110–117

Contents lists available at ScienceDirect

Diamond & Related Materials

journal homepage: www.elsevier.com/locate/diamond

Homogeneous and heterogeneous dislocation nucleation in diamond

Huizhen Yang[a], Jianwei Xiao[a], Ziwei Yao[b], Xiaoning Zhang[c], Fatima Younus[a], Roderick Melnik[d], Bin Wen[a,*]

[a] State Key Laboratory of Metastable Materials Science and Technology, Yanshan University, Qinhuangdao 066004, China
[b] School of Computer and Control Engineering, University of Chinese Academy of Sciences, Beijing, China
[c] School of Materials Science and Engineering, Bohai Shipbuilding Vocational College, Huludao 125105, China
[d] MS2 Discovery Interdisciplinary Research Institute, Wilfrid Laurier University, Waterloo 25, 75 University Ave. West, Ontario N2L 3C5, Canada

ARTICLE INFO

Keywords:
Diamond crystal
Simulation
Defects
Mechanical properties

ABSTRACT

Dislocation nucleation plays a key role in plastic deformation of diamond crystal. In this paper, homogeneous and heterogeneous nucleation nature for diamond $\frac{1}{6}\langle 112\rangle$ glide set dislocation and $\frac{1}{2}\langle 110\rangle$ shuffle set dislocation is studied by combining molecular dynamics method and continuum mechanics models. Our results show that although heterogeneous dislocation nucleation can decrease its activation energy, the activation energy at 0 GPa for diamond heterogeneous nucleation is still in the range of 100 eV. For $\frac{1}{6}\langle 112\rangle$ glide set and $\frac{1}{2}\langle 110\rangle$ shuffle set homogeneous nucleation, their critical nucleation shear stress approaches to diamond's ideal shear strength which implies that those dislocations do not nucleate before diamond structural instability only by a purely shearing manner. While for $\frac{1}{6}\langle 112\rangle$ glide set and $\frac{1}{2}\langle 110\rangle$ shuffle set heterogeneous nucleation, their critical nucleation shear stresses are 28.9 GPa and 48.2 GPa, these values are less than diamond's ideal shear strength which implies that these dislocations may be nucleated heterogeneously under certain shear stress condition. In addition, our results also indicate there exists a deformation mode transformation for diamond deformation behavior at strain rate of 10^{-3}/s. Our results provide a new insight into diamond dislocation nucleation and deformation.

1. Introduction

Diamond is the hardest, stiffest and least compressible crystalline material in the world that makes it fascinating to study scientifically as well as technologically important [1]. Therefore, a better understanding of mechanical properties of diamond is not only a foundational scientific issue, but also important for technological applications [2]. As a carrier of plastic deformation, dislocation is a crucial concept to understand material's mechanical properties [3–5]. For cubic diamond, two kinds of dislocations: $\frac{1}{6}\langle 112\rangle$ glide set partial dislocation (Shockley partial dislocation) and $\frac{1}{2}\langle 110\rangle$ shuffle set perfect dislocation dominate its plastic deformation [6–9]. Although dislocation mobility behavior for these two kinds of dislocations has been extensively studied by both experimental and computational methods [10–14], its nucleation process has been barely studied due to the difficulties in experimental methodologies and uncertain initial values in computer simulation and theoretical methods. With the development of computational capability and theoretical methods, the dislocation nucleation process can be put into effective operation [15–29].

Dislocation nucleation process is influenced by both athermal strength and thermal activation parameters. Theoretically, dislocation nucleation activation energy at a given thermal strength can be used to characterize dislocation nucleation nature [30]. To date, two methods can be used to obtain the activation energy for dislocation nucleation: one is based on the atomic simulation method [15, 16], and the other one on a continuum mechanics model [17–19]. For the atomistic simulation method, the activation energy can be obtained by searching Minimum Energy Path (MEP) method, such as Nudged-Elastic Band (NEB) [20, 22], Free-End Adaptive Nudged-Elastic Band (FEANEB) [21], string method [23] and direct Molecular Dynamics (MD) simulation [24] etc. For the continuum mechanics model, the dislocation nucleation activation energy can be deduced from the classical nucleation theory and continuous elastic theory [25]. In this case, the dislocation nucleation activation energy can be directly expressed as a function of dislocation loop radius, dislocation Burgers vector and materials elastic properties [19, 26–29].

In this work, homogeneous and heterogeneous nucleation nature for diamond $\frac{1}{6}\langle 112\rangle$ glide set dislocation and $\frac{1}{2}\langle 110\rangle$ shuffle set dislocation

* Corresponding author.
E-mail address: wenbin@ysu.edu.cn (B. Wen).

https://doi.org/10.1016/j.diamond.2018.07.005
Received 1 May 2018; Received in revised form 30 June 2018; Accepted 4 July 2018
Available online 07 July 2018
0925-9635/ © 2018 Elsevier B.V. All rights reserved.

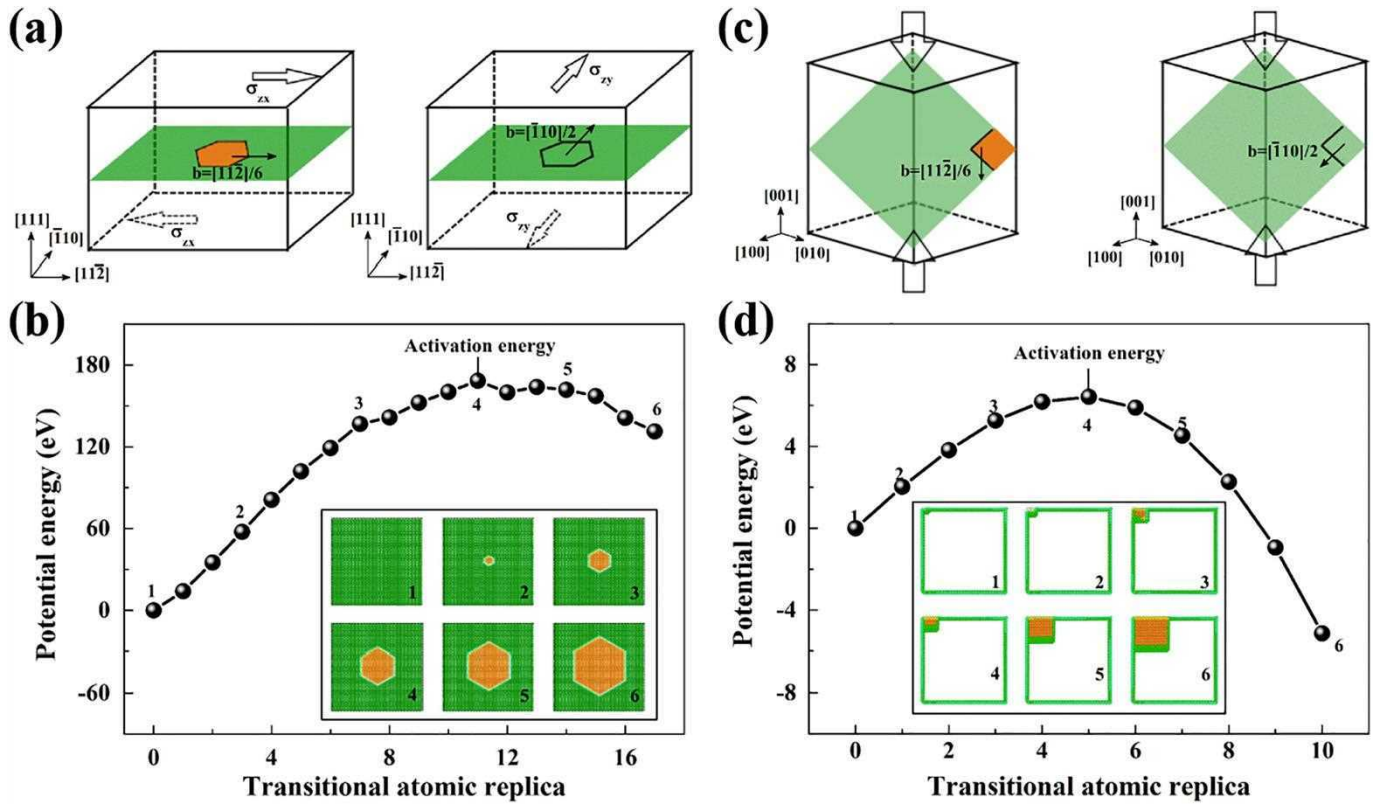

Fig. 1. (Color online) Schematic diagram of the geometric models for calculating diamond dislocation nucleation activation energy. (a) The models used for calculating homogeneous nucleation activation energy. Left and right models represent $\frac{1}{6}\langle 112\rangle$ glide set and $\frac{1}{2}\langle 110\rangle$ shuffle set dislocation nucleations, respectively. (c) The models used for calculating heterogeneous nucleation activation energy. Left and right models represent $\frac{1}{6}\langle 112\rangle$ glide set and $\frac{1}{2}\langle 110\rangle$ shuffle set dislocation nucleations, respectively. The relative potential energy as a function of dislocation loop sizes and the maximum energy is homogeneous (b) and heterogeneous (d) nucleation activation energy. The insert maps are the corresponding dislocation structures with different dislocation loop sizes. The stacking fault is marked in orange and the slip plane is marked in green.

is studied by combining MD method and continuum mechanics models. Our results indicate that although heterogeneous nucleation can reduce diamond dislocation nucleation activation energy, its activation energy is still in the range of 100 eV. For $\frac{1}{6}\langle 112\rangle$ glide set and $\frac{1}{2}\langle 110\rangle$ shuffle set heterogeneous nucleations, their critical nucleation shear stresses are 28.9 GPa and 48.2 GPa, these values are less than diamond's ideal shear strength which also implies that these dislocations may be nucleated heterogeneously under certain shear stress condition.

2. Computational methods

To simulate diamond nucleation process, a series of diamond supercells, which include a hexagonal dislocation with given size, were built. For the model used for homogeneous nucleation, a $131.1 \times 126.1 \times 61.78\,\text{Å}^3$ supercell containing ~180, 000 atoms was built and its x, y, and z axes were along $[11\bar{2}]$, $[\bar{1}10]$, and [111] directions (Fig. 1a), respectively. For the model used for heterogeneous nucleation, a $83.5 \times 83.5 \times 142.7\,\text{Å}^3$ supercell containing ~72, 000 atoms was built and its x, y and z axes were along [100], [010], and [001] directions (Fig. 1c), respectively. To build the dislocation structures in these models, atomic displacements were calculated by using the following equation [28, 31, 32]

$$u(x,y,z) = -\frac{\omega(x,y,z)}{4\pi}b, \tag{1}$$

where u is the displacement field for atom at position (x,y,z) and $\omega(x,y,z)$ is the solid angle associated with the polygonal dislocation loop [31]. Although only plastic displacement field was considered in this equation, elastic displacements of atoms arisen from dislocation could be obtained by next geometry optimization step.

In this work, MD simulation was performed by using the LAMMPS package [33] and the atomic interaction for carbon was modeled by the long-range bond-order potential (LCBOP) [34]. For homogeneous nucleation, periodic boundary conditions were imposed for three axes of simulation model, the elastic interaction between the primary dislocation loop and periodic images could be ignored because of the large enough diamond cells. For heterogeneous nucleation, the periodic boundary condition was imposed only in [001] direction, and the other directions were free of boundary conditions. In this MD simulation, shear stress and compressive stress were obtained by applying strain to computational models, time step was set at 1 fs and total simulation time was 30 ps. In the geometry optimization process, temperature was set to 0.001 K under NVT ensemble, the purpose was that this temperature was low enough to ensure that nucleation energy calculations were not corrupted by thermal motion of atoms. After geometry optimization, the diamond supercells with elastic and plastic displacements of atoms arisen from dislocation were obtained, and their total potential energy was obtained. By plotting potential energy as a function of dislocation size, dislocation nucleation activation energy was obtained (Fig. 1b and d). This computational method showed a possible and reasonable diamond dislocation nucleation path according to the characteristics of dislocation nucleation in the diamond structure materials.

In this paper, the elastic constants and Generalized Stacking Fault Energy (GSF) curves of diamond were calculated by using first principles method as implemented in the Vienna ab initio Simulation Package (VASP) [35, 36] and MD simulation. In this first principles calculation, the exchange-correlation energy was treated within the generalized

gradient approximation (GGA), and Projector-Augmented Wave (PAW) parameterization was used [37]. The calculated results of two simulated methods were almost identical (Supplementary Material Discussion S1).

3. Results and discussions

Diamond crystal can be described as two inter-penetrating face-centered-cubic (FCC) lattices with relative shifting of $\frac{1}{4}[111]$. Therefore, diamond crystal has two different (111) slip sets: a glide set and a shuffle set [38] (Fig. S1). Same as FCC metals, a perfect $\frac{1}{2}\langle 110\rangle$ diamond glide set dislocation often dissociates into two $\frac{1}{6}\langle 112\rangle$ glide set partial dislocations, bounding an area of stacking fault (SF). While for the diamond shuffle set dislocation, owing to the high unstable stacking fault energy, the diamond $\frac{1}{2}\langle 110\rangle$ shuffle set dislocation still exists in its perfect form without dissociation. Because of a large Peierls barrier with deep trough along ⟨110⟩ directions, diamond dislocation lies primarily along ⟨110⟩ directions. In this work, both homogeneous and heterogeneous dislocation nucleation processes for these two kinds of dislocations (e. g. $\frac{1}{6}\langle 112\rangle$ glide set dislocation and $\frac{1}{2}\langle 110\rangle$ shuffle set dislocation) along ⟨110⟩ direction are investigated.

3.1. Homogeneous nucleation of diamond $\frac{1}{6}\langle 112\rangle$ glide set dislocation

To study $\frac{1}{6}\langle 112\rangle$ glide set homogeneous dislocation nucleation, the activation energy under different resolved shear stresses is calculated by using MD simulation and they are plotted in Fig. 2a. As shown in Fig. 2a, when resolved shear stress increases from 14.7 to 35.9 GPa, its nucleation activation energy decreases from 168.4 to 28.5 eV. For comparison, activation energy of $\frac{1}{6}\langle 112\rangle$ glide set homogeneous dislocation nucleation for copper is calculated by MD simulation (detailed simulation methods are provided in Supplementary Material Discussion S2). The activation energy for copper decreases from 8.5 to 1.6 eV when resolved shear stress increases from 1.8 to 3.1 GPa (insert map of Fig. 2a), and they are 1–2 orders of magnitude lower than that of diamond. Many experimental and theoretical analyses indicate that the activation energy usually exhibits a nonlinear relationship with applied stress as the following [39]

$$Q_0(\tau) = B\left\{1 - \exp\left[\alpha\left(1 - \frac{\tau}{\tau_0}\right)\right]\right\}, \tag{2}$$

where Q_0 is nucleation activation energy, B and α are fitting parameters, τ_0 is critical stress.

By using Eq. (2) to fit our MD calculated nucleation activation energy data, the parameters in Eq. (2) are obtained, that is, $B = -0.0915$ eV, $\alpha = 8.8124$, $\tau_0 = 98.8$ GPa. The fitting correlation coefficient is 0.9920, which implies that fitting results are reliable. The fitted activation energy is 614.6 eV under 0 GPa condition (Table 1), and the fitted critical stress of 98.8 GPa approaches to diamond ideal shear strength [40, 41]. For copper, the fitting parameters in Eq. (2) are $B = -0.0915$ eV, $\alpha = 8.8124$, and the fitting correlation coefficient is 0.9983. The critical stress is 3.8 GPa, and it is about 1/25 of critical stress for diamond nucleation.

By calculating negative derivative of the activation energy with respect to applied shear stress, the activation volume can be obtained and expressed as

$$\Omega = \frac{B\alpha}{\tau_0}\exp\left[\alpha\left(1 - \frac{\tau}{\tau_0}\right)\right], \tag{3}$$

where Ω is activation volume, B, α and τ_0 are fitted parameters from Eq. (2).

By using Eq. (3), the relationship between activation volume and resolved shear stress for diamond and copper is calculated and shown in Fig. 2b. For diamond, the activation volume is 2869 b^3 at 0 GPa condition (Table 1). When resolved shear stress increases from zero to its critical stress value (98.8 GPa), the activation volume decreases uniformly and finally becomes zero. For copper, when resolved shear stress increases from 0 GPa to critical stress value (3.8 GPa), the activation volume decreases from 7078 to 0 b^3, and these results agree well with experimental values of 100–1000 b^3 [42].

Diamond has almost 10 times higher shear modulus than that of general metal materials. Meanwhile, its stacking fault energy is roughly the same as that of metal materials [43–45]. This elastic property difference between diamond and metal materials may lead to a great difference in their $\frac{1}{6}\langle 112\rangle$ glide set dislocation nucleation behavior. To

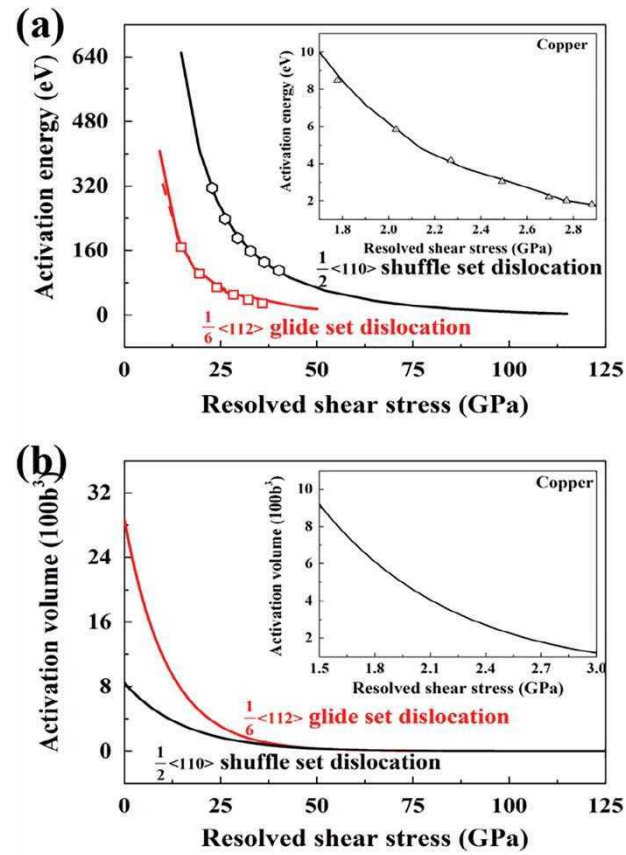

Fig. 2. (Color online) Stress dependent activation energy and activation volume for diamond homogeneous dislocation nucleation. (a) The activation energy as a function of resolved shear stress for diamond $\frac{1}{6}\langle 112\rangle$ glide set dislocation and $\frac{1}{2}\langle 110\rangle$ shuffle set homogeneous dislocation nucleation. Insert map is the activation energy as a function of resolved shear stress for copper $\frac{1}{6}\langle 112\rangle$ glide set homogeneous dislocation nucleation. Input parameters, calculated by MD and first principles in the model, are both used to calculate activation energy, their results are marked by dash lines and lines, respectively. Symbols are MD results. (b) The activation volume as a function of resolved shear stress for diamond $\frac{1}{6}\langle 112\rangle$ glide set dislocation and $\frac{1}{2}\langle 110\rangle$ shuffle set homogeneous dislocation nucleation. Insert map is the activation volume as a function of resolved shear stress for copper $\frac{1}{6}\langle 112\rangle$ glide set homogeneous dislocation nucleation.

Table 1
Activation energy Q_0 (0 GPa), activation volume Ω (0 GPa) and critical nucleation stress σ for diamond dislocation nucleation.

Nucleation type	Dislocation type	Q_0 (eV)	Ω (b^3)	σ (GPa)
Homogeneous nucleation	$\frac{1}{6}\langle 112\rangle$ glide set	614.6	2869	98.8
	$\frac{1}{2}\langle 110\rangle$ shuffle set	1320.9	844	117.4
Heterogeneous nucleation	$\frac{1}{6}\langle 112\rangle$ glide set	298.8	2183	28.9
	$\frac{1}{2}\langle 110\rangle$ shuffle set	709.0	317	48.2

gain an insight in this issue, the dislocation nucleation activation energy was investigated by using a continuum mechanics model. In this continuum mechanics model, the dislocation energy can be expressed as [15]

$$E(b_f, A; \tau) = \int_{-\frac{\delta}{2}}^{\frac{\delta}{2}} \frac{\mu {b_f}^2}{4\pi(1-\nu)}[1-\nu\cos^2\theta]R\ln\frac{R}{a}d\psi + [\gamma_{GSF}(b_f+u_0;\tau)-\gamma_{GSF}(u_0;\tau)]A - A\tau b_f, \quad (4)$$

where the first, second and third parts of this model represent elastic energy (EE), stacking fault energy (SFE) and work done by stress (WD), respectively. τ is resolved shear stress, b_f is the fraction Burgers vector of partial dislocation, γ_{GSF} is the generalized stacking fault energy under different shear stress, R is the dislocation loop radius, δ is the included angle of the nucleating dislocation arc, A is the nucleation area that $A = \frac{1}{2}\delta R^2$, μ is shear modulus, ν is Poisson's ratio, a is the dislocation core cut-off radius, θ is the angle between direction of b_f and dislocation line (here $\theta = \psi$). By taking the maximum of $E_b(\tau) = \max_A E(A;\tau)$, the activation energy under a resolved shear stress can be obtained.

Taking diamond $\frac{1}{6}\langle 112\rangle$ glide set homogeneous dislocation nucleation activation energy as an example, EE, SFE and WD change with increasing dislocation loop radius at a constant resolved shear stress as shown in Fig. 3a. EE is in a linear relationship with dislocation loop radius, while SFE and WD exhibit a square relationship with dislocation loop radius. This leads to the maximum dislocation energy (i. e. nucleation activation energy) which exists at a critical nucleation radius.

By using this continuum mechanics model (the parameters used are calculated by MD and first principles, details in Table 2, Discussion S3 and Figs. S2–S3), the activation energy for diamond $\frac{1}{6}\langle 112\rangle$ glide set homogeneous dislocation nucleation is calculated, and plotted in Fig. 2a. For the model, its input parameters calculated by MD and first principles agree well with each other. As can be seen in Fig. 2a, the nucleation activation energy predicted from continuum mechanics model agree well with MD calculated results. This indicates the model is suitable for predicting diamond $\frac{1}{6}\langle 112\rangle$ glide set homogeneous dislocation nucleation.

To gain an insight into diamond $\frac{1}{6}\langle 112\rangle$ glide set homogeneous dislocation nucleation activation energy compositions and their contributions to nucleation activation energy, the energy contribution to nucleation activation energy is investigated, and plotted in Fig. 3c. In this work, the contributions of each part to activation energy are defined by ratio of each part and activation energy. The values calculated

Table 2
Parameters used in continuum mechanics model for diamond dislocation nucleation, shear modulus μ, Poisson's ratio ν, angle of dislocation arc θ and dislocation core cut off a.

Nucleation type	Dislocation type	μ (GPa)	ν	θ (°)	a (Å)
Homogeneous nucleation	$\frac{1}{6}\langle 112\rangle$ glide set	515.0	0.1043	360	1.70
	$\frac{1}{2}\langle 110\rangle$ shuffle set			360	0.80
Heterogeneous nucleation	$\frac{1}{6}\langle 112\rangle$ glide set			120	1.09
	$\frac{1}{2}\langle 110\rangle$ shuffle set			120	1.26

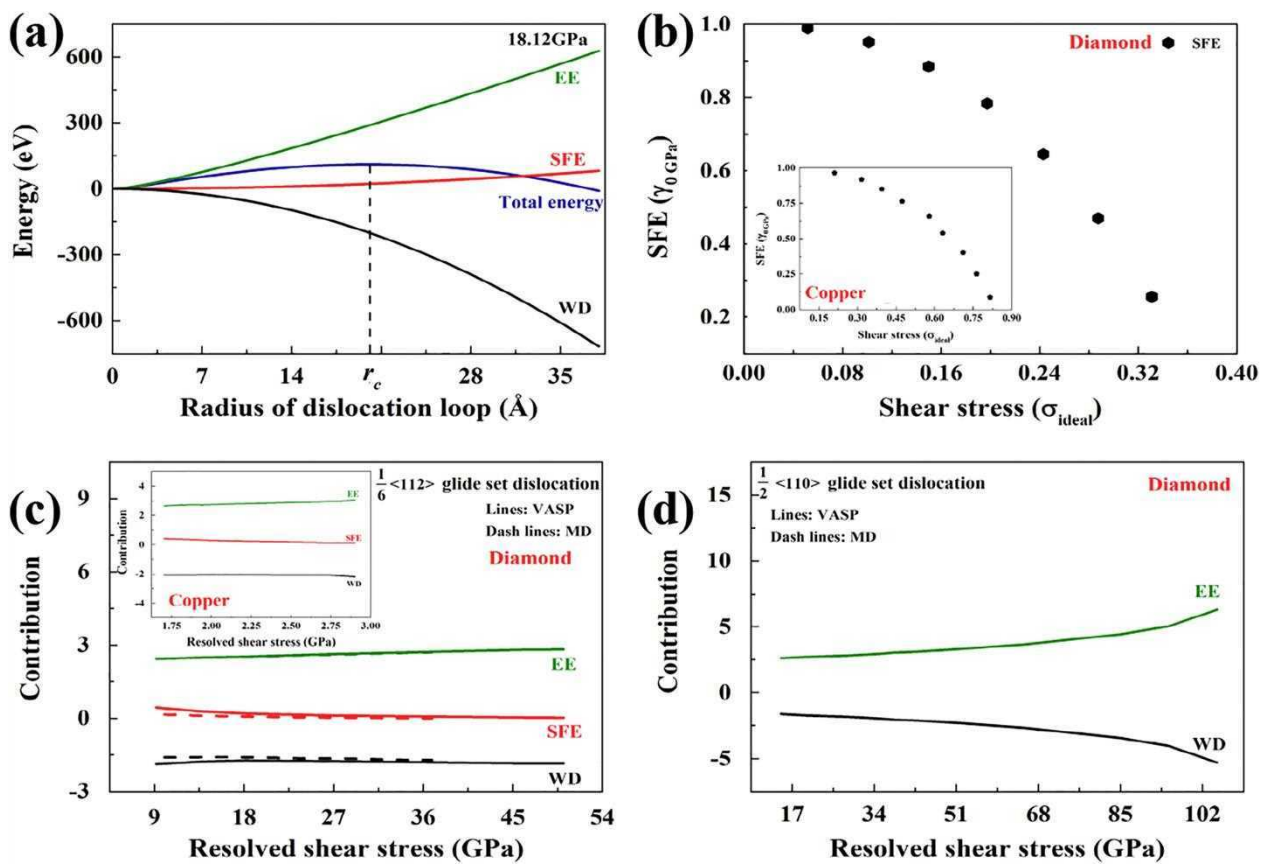

Fig. 3. (Color online) Diamond homogeneous dislocation nucleation activation energy and its components calculated by continuum mechanics model. (a) Dislocation energy change with changing radius of dislocation loop. **EE** is elastic energy, **SFE** is stacking fault energy, **WD** is work done by stress, r_c represents critical nucleation radius. (b) Stress dependent SFE for diamond. Insert map is shear stress dependent SFE for copper. (c) Stress dependent three parts of energy contributions to the activation energy for diamond $\frac{1}{6}\langle 112\rangle$ glide set homogeneous dislocation nucleation. Insert map is stress dependent three parts of energy contributions to the activation energy for copper $\frac{1}{6}\langle 112\rangle$ glide set dislocation nucleation. (d) Stress dependent three parts of energy contributions to the activation energy for diamond $\frac{1}{2}\langle 110\rangle$ shuffle set homogeneous dislocation nucleation.

according to input parameters in model are consistent for both MD and first principles.

As shown in Fig. 3c, the contribution of SFE to diamond $\frac{1}{6}\langle 112\rangle$ glide set dislocation nucleation activation energy decreases from 0.16 to 0.001 as resolved shear stress increases from 5.1 to 30 GPa, and decreases from 0.46 to 0.05 for copper (resolved shear stress increases from 0.2 to 2.9 GPa) (insert map of Fig. 3c). This shows the less contribution of SFE to activation energy when resolved shear stress is increased, EE and WD contribute to activation energy more. WD is a linearly increasing function with respect to resolved shear stress, but EE is only a function of nucleation radius. This leads to the decrease in critical nucleation radius (or nucleation activation volume) with increase in resolved shear stress, making less contribution of SFE to nucleation activation energy. The activation volume of diamond $\frac{1}{6}\langle 112\rangle$ glide set homogeneous dislocation nucleation is of the same order of magnitude as copper, which means that both materials have a similar activation area, but their shear moduli is ten times in difference. This difference causes the SFE of diamond to be zero as resolved shear stress increases to 40 GPa (critical stress is 98.8 GPa), but that of copper reduces about 75% when resolved shear stress increases to 2.9 GPa (close to critical stress) (Fig. 3b). Thus, higher shear modulus of diamond causes higher activation energy and lower influence of SFE on activation energy than that of copper. Furthermore, because diamond has higher nucleation activation energy, it needs high enough resolved shear stress to nucleate. In this case, SFE is hardly influential during the process of diamond dislocation nucleation. However, for copper, its nucleation activation energy is much lower than that of diamond. Its dislocation can nucleate under much lower resolved shear stress by the aid of thermal vibration. This also leads to the point that SFE has significant influence on the process of copper dislocation nucleation.

3.2. Homogeneous nucleation of diamond $\frac{1}{2}\langle 110\rangle$ shuffle set dislocation

To study homogeneous nucleation nature of diamond $\frac{1}{2}\langle 110\rangle$ shuffle set dislocation, the activation energy under different shear stresses is calculated by MD simulation. As shown in Fig. 2a, the activation energy decreases from 315.3 to 110.6 eV when resolved shear stress increases from 22.8 to 40.2 GPa. These results are almost 4 times larger than that of $\frac{1}{6}\langle 112\rangle$ glide set homogeneous dislocation nucleation under the same stress conditions.

In the same way as in the method used in Section 3.1, the nucleation activation parameters for $\frac{1}{2}\langle 110\rangle$ shuffle set homogeneous dislocation nucleation are deduced by using Eqs. (2) and (3) to fit the MD simulation results, they are plotted in Fig. 2b and Table 1. Like $\frac{1}{6}\langle 112\rangle$ glide set homogeneous dislocation nucleation, the obtained critical nucleation stress for $\frac{1}{2}\langle 110\rangle$ shuffle set dislocation nucleation approaches to diamond ideal shear strength [40, 41]. This implies that these two kinds of dislocations cannot nucleate homogeneously before diamond structural instability only by a purely shearing manner. This activation volume under 0 GPa condition is about 1/3 of activation volume for diamond $\frac{1}{6}\langle 112\rangle$ glide set homogeneous dislocation nucleation.

To study the diamond $\frac{1}{2}\langle 110\rangle$ shuffle set homogeneous dislocation nucleation nature further, the continuum mechanics model, as expressed in Eq. (4), is also used to study the contribution of each part to nucleation activation energy. $\frac{1}{2}\langle 110\rangle$ shuffle set dislocation is a perfect dislocation. Its nucleation cannot produce additional stacking fault. Therefore, the second part in Eq. (4) can be omitted. The parameters used in Eq. (4) are listed in Table 2. The calculated nucleation activation energy (in Fig. 2a) by the continuum mechanics model agrees well with our MD simulation results, indicating that this model is also reliable for diamond $\frac{1}{2}\langle 110\rangle$ shuffle set dislocation nucleation. The contributions of EE and WD to nucleation activation energy are shown in Fig. 3d.

As shown in Fig. 3d, when resolved shear stress increases from 14.7 to 105.0 GPa, the contribution of EE to activation energy increases from

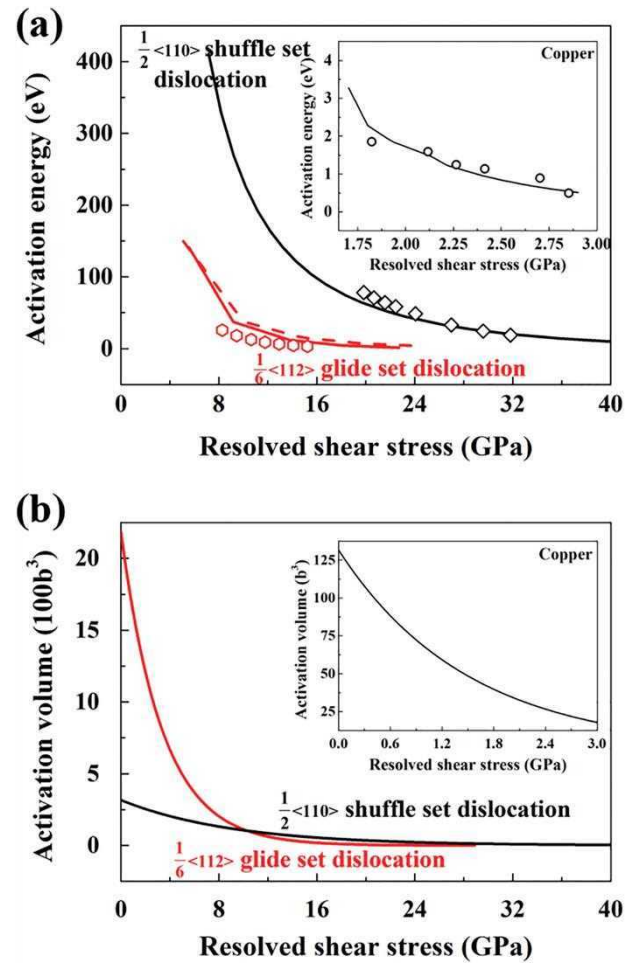

Fig. 4. (Color online) Stress dependent activation energy and activation volume for diamond heterogeneous dislocation nucleation. (a) Activation energy as a function of resolved shear stress for diamond $\frac{1}{6}\langle 112\rangle$ glide set and $\frac{1}{2}\langle 110\rangle$ shuffle set heterogeneous dislocation nucleations. Insert map is the activation energy as a function of resolved shear stress for copper $\frac{1}{6}\langle 112\rangle$ glide set homogeneous dislocation nucleation. Input parameters, calculated by MD and first principles in the model, are both used to calculate activation energy, their results are marked by dash lines and lines, respectively. Symbols are MD results. (b) The activation volume as a function of resolved shear stress for diamond $\frac{1}{6}\langle 112\rangle$ glide set dislocation and $\frac{1}{2}\langle 110\rangle$ shuffle set homogeneous dislocation nucleation. Insert map is the activation volume as a function of resolved shear stress for copper $\frac{1}{6}\langle 112\rangle$ glide set homogeneous dislocation nucleation.

2.62 to 6.30, while the contribution of WD negatively increases from −1.62 to −5.30. The ratio of EE to WD decreases from 1.62 to 1.19 (Fig. S4). This indicates that EE has more effects on activation in $\frac{1}{2}\langle 110\rangle$ shuffle set homogeneous dislocation nucleation process. The continuum mechanics model used here demonstrates that WD is a linearly increasing function with respect to resolved shear stress, but EE is only a function of nucleation radius. Thus, with increase of resolved shear stress, the role of WD becomes more pronounced.

3.3. Heterogeneous nucleation of diamond $\frac{1}{6}\langle 112\rangle$ glide set dislocation

It is demonstrated that homogeneous dislocation nucleation can barely occur in diamond. Recall now that some works show that dislocation is easier to form on crystal defect positions than in perfect crystals [46–48]. In this section, heterogeneous nucleation nature for diamond $\frac{1}{6}\langle 112\rangle$ glide set dislocation is studied. The computational model used in this simulation is shown in Fig. 1c. The dislocation nucleation activation energy is calculated by MD simulation and they are

plotted in Fig. 4a.

As shown in Fig. 4a, when resolved shear stress increases from 8.3 to 15.2 GPa, activation energy for diamond dislocation nucleation decreases from 25.7 to 3.3 eV. In insert map of Fig. 4a, when resolved shear stress increases from 1.8 to 2.9 GPa, activation energy for copper $\frac{1}{6}\langle 112\rangle$ glide set heterogeneous dislocation nucleation decreases from 1.9 to 0.5 eV, its activation energy is much lower than that of diamond.

For diamond $\frac{1}{6}\langle 112\rangle$ glide set dislocation nucleation, its fitted activation energy at 0 GPa is 298.8 eV and critical nucleation stress is 28.9 GPa by using Eq. (2) (listed in Table 1). Critical nucleation stress for diamond is about 8 times that of copper (fitted critical nucleation stress is 3.5 GPa). The activation volume of diamond is obtained by Eq. (3) and plotted in Fig. 4b. When resolved shear stress increases from 0 GPa to critical nucleation stress (28.9 GPa), the activation volume decreases from 2183 to 0 b^3. The activation volume under 0 GPa for diamond heterogeneous dislocation nucleation is little lower than homogeneous nucleation one (2869 b^3), and much larger than that of copper (132 to 12 b^3).

The continuum mechanics model mentioned above is also used to calculate heterogeneous nucleation activation energy. The used parameters are listed in Table 2. The calculated activation energy under different resolved shear stress is shown in Fig. 4a. The results show that model calculated results agree well with MD simulation results. To quantitatively analyze contributions of each part to nucleation activation energy, each part of activation energy is separately calculated, and they are plotted in Fig. 5a.

Fig. 5a shows the contribution of SFE to activation energy for diamond $\frac{1}{6}\langle 112\rangle$ glide set heterogeneous dislocation nucleation, this value decreases from 0.40 to 0.09 (stress range is 5.1 to 24.0 GPa). In insert map of Fig. 5a, the contribution of SFE to activation energy for copper decreases from 0.54 to 0.08 (stress range is 1.2 to 2.9 GPa). The variation in relationship between these parameters and resolved shear stress is similar to that of homogeneous dislocation nucleation which we have mentioned earlier. These results show that the contribution of SFE to activation energy for diamond $\frac{1}{6}\langle 112\rangle$ glide set heterogeneous nucleation is little lower than copper $\frac{1}{6}\langle 112\rangle$ glide set heterogeneous nucleation. From MD results, activation volume of diamond glide set heterogeneous nucleation is nearly 15 times larger than that of copper. This may cause the contribution of SFE to activation energy for diamond heterogeneous nucleation to be closer to copper, but the higher shear modulus of diamond still leads to a value which is lower than copper. After the combined analyses of diamond and copper $\frac{1}{6}\langle 112\rangle$ glide set homogeneous dislocation nucleation, we find higher shear modulus of diamond compared to that of copper which results in diamond's much higher activation energy and lower SFE' contribution to activation energy. Besides, combining the homogeneous nucleation results for diamond and copper $\frac{1}{6}\langle 112\rangle$ glide set dislocations, we also obtain that due to the high bond strength of sp^3 C—C bond in diamond, the activation energy of dislocation nucleation in diamond is much higher than that of dislocation nucleation in copper.

3.4. Heterogeneous nucleation of diamond $\frac{1}{2}\langle 110\rangle$ shuffle set dislocation

The activation energy of diamond $\frac{1}{2}\langle 110\rangle$ shuffle set heterogeneous dislocation nucleation under different resolved shear stresses is calculated by MD simulation. The used model is shown in Fig. 1c and MD calculated results are plotted in Fig. 4a. As shown in Fig. 4a, when resolved shear stress increases from 19.8 to 31.8 GPa, nucleation activation energy decreases from 78.0 to 18.8 eV. They are nearly 1/10–1/4 that of $\frac{1}{2}\langle 110\rangle$ shuffle set homogeneous dislocation nucleation under the same stress condition.

By using Eqs. (2) and (3) to fit MD calculated results, the activation energy (0 GPa), critical nucleation stress and activation volume are obtained, they are listed in Table 1. Fig. 4b shows the dependence of resolved shear stress on activation volume. According to these results, the fitted critical nucleation stress is 48.2 GPa, it is about 2/5 times that of $\frac{1}{2}\langle 110\rangle$ shuffle set homogeneous dislocation nucleation. The activation volume is 317 b^3 (0 GPa), it is about 1/3 of activation volume for $\frac{1}{2}\langle 110\rangle$ shuffle set homogeneous dislocation nucleation.

To further study diamond $\frac{1}{2}\langle 110\rangle$ shuffle set heterogeneous dislocation nucleation nature, the contribution of each part to nucleation activation energy is also studied by using the continuum mechanics model as expressed in Eq. (4). Parameters used in model are listed in Table 2. The calculated nucleation activation energy is shown in Fig. 4a. The results agree well with MD simulation results. The contributions of EE and WD to nucleation activation energy are plotted in Fig. 5b. In Fig. 5b, when resolved shear stress increases from 7.2 to 40.0 GPa, the contribution of EE to activation energy increases from 2.65 to 4.69 and absolute value for the contribution of WD to activation energy increases from 1.65 to 3.69. Apparently, like $\frac{1}{2}\langle 110\rangle$ shuffle set homogeneous dislocation nucleation, EE plays a key role in activation energy. Fig. S4 shows that the ratio (absolute value) of EE and WD for heterogeneous nucleation is lower than that for homogeneous nucleation. This difference indicates that the effect of EE on activation reduces in $\frac{1}{2}\langle 110\rangle$ shuffle set heterogeneous dislocation nucleation process, and this change may influence the magnitude of heterogeneous nucleation

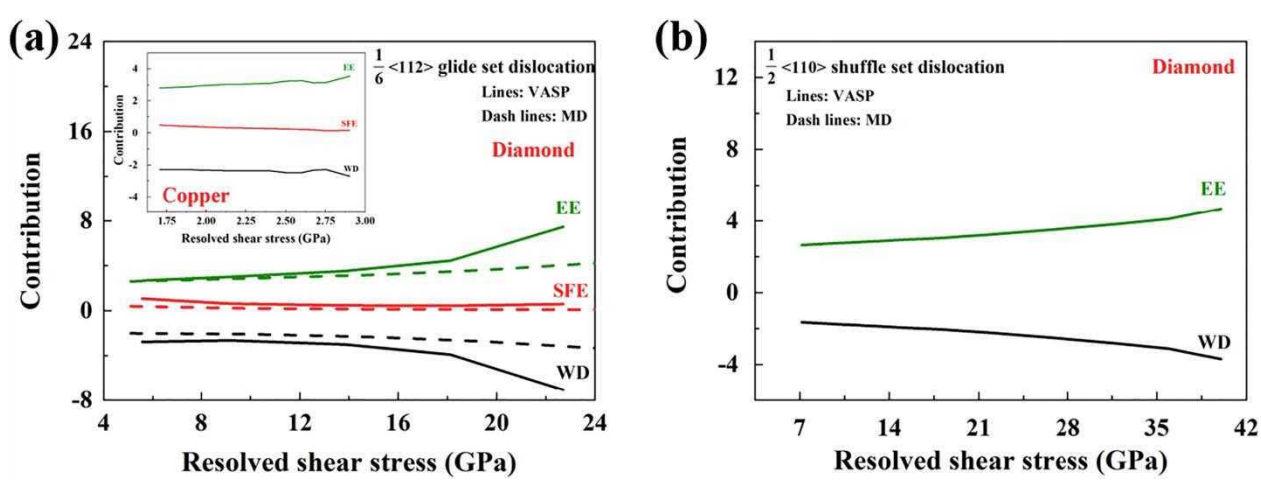

Fig. 5. (Color online) Diamond heterogeneous dislocation nucleation components calculated by continuum mechanics model. (a) Stress dependent three parts of energy contributions to the activation energy for diamond $\frac{1}{6}\langle 112\rangle$ glide set dislocation heterogeneous nucleation. Insert map is stress dependent three parts energy contributions on activation energy for copper $\frac{1}{6}\langle 112\rangle$ glide set dislocation nucleation. (b) Stress dependent three parts energy contributions on activation energy for diamond $\frac{1}{2}\langle 110\rangle$ shuffle set dislocation heterogeneous nucleation.

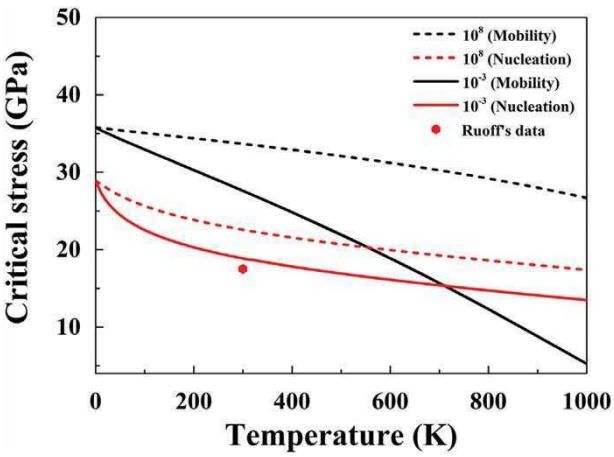

Fig. 6. (Color online) Temperature and strain rate dependent critical stress for diamond dislocation nucleation and mobility. Red represents diamond $\frac{1}{6}\langle 112\rangle$ glide set heterogeneous dislocation nucleation and black represents diamond dislocation moving on 2° twist grain boundary (TGB).

activation energy.

Based on MD results of diamond $\frac{1}{6}\langle 112\rangle$ glide set and $\frac{1}{2}\langle 110\rangle$ shuffle set homogeneous and heterogeneous dislocation nucleation, heterogeneous nucleation activation volume is lower than that of homogeneous nucleation because heterogeneous nucleation's radius is much smaller. Under the same stress conditions, smaller nucleation radius for heterogeneous nucleation causes reduction of each part of activation energy. Furthermore, heterogeneous nucleation occurs in corners making its dislocation length and area part of homogeneous nucleation dislocation length. Thus energy of heterogeneous dislocation nucleation decreases. All these observations indicate that heterogeneous nucleation has a lower activation energy compared to that of homogeneous nucleation.

3.5. Dislocation nucleation competes with dislocation mobility

For a realistic diamond crystal, when it is subjected to an applied stress, dislocation nucleation and mobility will take place. To study the competition between dislocation nucleation and mobility, their critical stress under different temperatures and strain rates are compared.

For dislocation nucleation, temperature and strain rate dependent critical stress is calculated by using the following equation [30, 49]

$$\frac{Q(\tau,T)}{\kappa_B T} = \ln\frac{\kappa_B T N \nu_0}{E_Y \dot{\varepsilon}\Omega(\tau,T)}, \tag{5}$$

where ν_0 is the attempt frequency, κ_B is Boltzmann constant, $\dot{\varepsilon}$ is strain rate, N is the number of equivalent nucleation sites, E_Y is Young's modulus, $Q(\tau,T)$ is activation energy under conditions of applied shear stress and temperature. Here, $Q(\tau,T) = (1 - T/T_m)Q_0(\tau)$, T_m is the surface disordering temperature, $Q_0(\tau)$ is the activation energy under athermal condition. The activation volume $\Omega(\tau,T) = (1 - T/T_m)\Omega_0(\tau)$, here $\Omega_0 \equiv -dQ_0/d\tau$.

By using Eq. (5), temperature dependent critical nucleation stress under strain rate of $\dot{\varepsilon} = 10^8/s$ and $\dot{\varepsilon} = 10^{-3}/s$ for diamond $\frac{1}{6}\langle 112\rangle$ glide set heterogeneous dislocation nucleation (it has the lowest activation energy among all four dislocation nucleation types studied in this work) is calculated and they are plotted in Fig. 6.

For dislocation mobility, temperature and strain rate dependent critical stress is calculated by using the following equation [50]

$$\dot{\varepsilon} = \frac{\rho b a L \nu_0}{w}\exp\left(-\frac{Q(\tau,T)}{\kappa_B T}\right), \tag{6}$$

where ρ is dislocation density, b is Burgers vector, a is the spacing that the entire dislocation line moves to the next position, L is the length of dislocation line, w is the width of dislocation kink.

By using Eq. (6) (MD results for dislocation moving on 2° twist grain boundary (TGB) are shown in Figs. S5–S7), temperature dependent critical stress under strain rate of $\dot{\varepsilon} = 10^8/s$ and $\dot{\varepsilon} = 10^{-3}/s$ for dislocation moving on 2° twist grain boundary (TGB) (its activation energy is the lowest among dislocations moving on and penetrating TGB) is calculated and they are plotted in Fig. 6.

As shown in Fig. 6, the critical stress for diamond dislocation nucleation and mobility decreases significantly with increase in temperature at a constant strain rate. At temperature of 300 K and strain rate of $10^{-3}/s$, the critical stress for diamond plastic deformation is equal to 19 GPa according to the glide set heterogeneous nucleation. These values agree with previous experimental value of 17 GPa [51] data and further confirm the parameters and model used in this work are reliable. At $\dot{\varepsilon} = 10^8/s$, critical nucleation stress for dislocation nucleation is lower than dislocation mobility at temperature range from 0 to 1000 K. What is even more noteworthy is that when strain rate is $\dot{\varepsilon} = 10^{-3}/s$, there exists a crossing point for dislocation nucleation and mobility critical stress curves. This implies that there is a deformation mode transformation between the dislocation nucleation dominating case and the dislocation mobility dominating case. When the temperature is above 710 K, dislocation mobility dominates diamond plastic deformation. When the temperature is below 710 K, dislocation nucleation dominates diamond plastic deformation.

4. Conclusions

In summary, homogeneous and heterogeneous nucleation nature for diamond $\frac{1}{6}\langle 112\rangle$ glide set dislocation and $\frac{1}{2}\langle 110\rangle$ shuffle set dislocation were studied by combining molecular dynamics method and continuum mechanics models. Our results illustrate that although heterogeneous dislocation nucleation can decrease its activation energy, the activation energy at 0 GPa for diamond heterogeneous nucleation is still in the range of 100 eV. For $\frac{1}{6}\langle 112\rangle$ glide set and $\frac{1}{2}\langle 110\rangle$ shuffle set homogeneous nucleation, their critical stress approaches to diamond's ideal shear strength. While for $\frac{1}{6}\langle 112\rangle$ glide set and $\frac{1}{2}\langle 110\rangle$ shuffle set heterogeneous nucleation, their critical stresses are 28.9 GPa and 48.2 GPa, these values are less than diamond's ideal shear strength. In addition, there exists a deformation mode transformation for diamond deformation behavior at strain rate of $\dot{\varepsilon} = 10^{-3}/s$. When the temperature is above 710 K, dislocation mobility dominates diamond plastic deformation. When the temperature is below 710 K, dislocation nucleation dominates diamond plastic deformation. This study provides a new insight into diamond nucleation and deformation mechanism and it provides important reference values for the experiments analyzing diamond mechanical properties.

Acknowledgments

This work was supported by the National Natural Science Foundation of China (Grant No. 51771165, 51372215). R.M. acknowledges the support from the NSERC and CRC programs, Canada.

Appendix A. Supplementary data

Supplementary data to this article can be found online at https://doi.org/10.1016/j.diamond.2018.07.005.

References

[1] J.E. Field, The Properties of Diamond, Academic Press, 1979.
[2] Q. Huang, D. Yu, B. Xu, W. Hu, Y. Ma, Y. Wang, Z. Zhao, B. Wen, J. He, Z. Liu, Y. Tian, Nanotwinned diamond with unprecedented hardness and stability, Nature 510 (7504) (2014) 250–253.
[3] M. Tang, J. Marian, Temperature and high strain rate dependence of tensile deformation behavior in single-crystal iron from dislocation dynamics simulations, Acta Mater. 70 (15) (2014) 123–129.

[4] S. Shao, J. Wang, I.J. Beyerlein, A. Misra, Glide dislocation nucleation from dislocation nodes at semi-coherent {111} Cu–Ni interfaces, Acta Mater. 98 (2015) 206–220.
[5] J.A. Elawady, Unravelling the physics of size-dependent dislocation-mediated plasticity, Nat. Commun. 6 (2015) 5926.
[6] C. Brookes, Plastic deformation and anisotropy in the hardness of diamond, Nature 228 (5272) (1970) 660–661.
[7] H.-J. Möller, The movement of dissociated dislocations in the diamond-cubic structure, Acta Metall. 26 (6) (1978) 963–973.
[8] A. Argon, P. Haasen, A new mechanism of work hardening in the late stages of large strain plastic flow in fcc and diamond cubic crystals, Acta Metall. Mater. 41 (11) (1993) 3289–3306.
[9] I.N. Remediakis, G. Kopidakis, P.C. Kelires, Softening of ultra-nanocrystalline diamond at low grain sizes, Acta Mater. 56 (18) (2008) 5340–5344.
[10] A.T. Blumenau, R. Jones, T. Frauenheim, B. Willems, O.I. Lebedev, G. Van Tendeloo, D. Fisher, P.M. Martineau, Dislocations in diamond: dissociation into partials and their glide motion, Phys. Rev. B 68 (1) (2003) 366–369.
[11] R.a.T.F.A.T. Blumenau, The 60° dislocation in diamond and its dissociation, J. Phys. Condens. Matter 15 (39) (2003) S2951.
[12] N. Fujita, A.T. Blumenau, R. Jones, S. Öberg, P.R. Briddon, Theoretical studies on ⟨100⟩ dislocations in single crystal CVD diamond, Phys. Status Solidi A 203 (12) (2006) 3070–3075.
[13] P. Martineau, M. Gaukroger, R. Khan, D. Evans, Effect of steps on dislocations in CVD diamond grown on {001} substrates, Phys. Status Solidi A 6 (8) (2009) 1953–1957.
[14] D. Rodney, L. Ventelon, E. Clouet, L. Pizzagalli, F. Willaime, Ab initio modeling of dislocation core properties in metals and semiconductors, Acta Mater. 124 (2017) 633–659.
[15] E. Rabkin, H.S. Nam, D. Srolovitz, Atomistic simulation of the deformation of gold nanopillars, Acta Mater. 55 (6) (2007) 2085–2099.
[16] M. Yaghoobi, G.Z. Voyiadjis, Size effects in fcc crystals during the high rate compression test, Acta Mater. 121 (2016) 190–201.
[17] G. Xu, A.S. Argon, Homogeneous nucleation of dislocation loops under stress in perfect crystals, Philos. Mag. Lett. 80 (9) (2000) 605–611.
[18] M. De Koning, W. Cai, V.V. Bulatov, Anomalous dislocation multiplication in FCC metals, Phys. Rev. Lett. 91 (2) (2003) 025503.
[19] P. Gu, M. Dao, R.J. Asaro, S. Suresh, A unified mechanistic model for size-dependent deformation in nanocrystalline and nanotwinned metals, Acta Mater. 59 (18) (2011) 6861–6868.
[20] G. Henkelman, H. Jónsson, Improved tangent estimate in the nudged elastic band method for finding minimum energy paths and saddle points, J. Chem. Phys. 113 (22) (2000) 9978–9985.
[21] J. Zhang, H. Zhang, H. Ye, Y. Zheng, Free-end adaptive nudged elastic band method for locating transition states in minimum energy path calculation, J. Chem. Phys. 145 (9) (2016) 094104.
[22] G. Henkelman, B.P. Uberuaga, H. Jónsson, A climbing image nudged elastic band method for finding saddle points and minimum energy paths, J. Chem. Phys. 113 (22) (2000) 9901–9904.
[23] E. Weinan, W. Ren, E. Vanden-Eijnden, String method for the study of rare events, Phys. Rev. B 66 (5) (2002) 052301.
[24] P. Hirel, J. Godet, S. Brochard, L. Pizzagalli, P. Beauchamp, Determination of activation parameters for dislocation formation from a surface in fcc metals by atomistic simulations, Phys. Rev. B 78 (6) (2008) 064109.
[25] P. Hänggi, P. Talkner, M. Borkovec, Reaction-rate theory: fifty years after Kramers, Rev. Mod. Phys. 62 (2) (1990) 251.
[26] R. Scattergood, D. Bacon, The Orowan mechanism in anisotropic crystals, Philos. Mag. 31 (1) (1975) 179–198.
[27] Y. Xiang, H. Wei, P. Ming, E. Weinan, A generalized Peierls–Nabarro model for curved dislocations and core structures of dislocation loops in Al and Cu, Acta Mater. 56 (7) (2008) 1447–1460.
[28] K. Kang, Atomistic Modelling of Fracture Mechanisms in Semiconductor Nanowires under Tension, Stanford University, 2011.
[29] K.K. Sylvie Aubry, Seunghwa Ryu, Wei Cai, Energy barrier for homogeneous dislocation nucleation comparing atomistic and continuum models, Scr. Mater. 64 (11) (2011) 1043–1046.
[30] T. Zhu, J. Li, A. Samanta, A. Leach, K. Gall, Temperature and strain-rate dependence of surface dislocation nucleation, Phys. Rev. Lett. 100 (2) (2008) 025502.
[31] D.M. Barnett, The displacement field of a triangular dislocation loop, Philos. Mag. A 51 (3) (2006) 383–387.
[32] D.M. Barnett, R.W. Balluffi, The displacement field of a triangular dislocation loop–a correction with commentary, Philos. Mag. Lett. 87 (12) (2007) 943–944.
[33] S. Plimpton, Fast parallel algorithms for short-range molecular dynamics, J. Comput. Phys. 117 (1) (1995) 1–19.
[34] J. Los, A. Fasolino, Intrinsic long-range bond-order potential for carbon: performance in Monte Carlo simulations of graphitization, Phys. Rev. B 68 (2) (2003) 024107.
[35] J.P. Perdew, M. Ernzerhof, K. Burke, Rationale for mixing exact exchange with density functional approximations, J. Chem. Phys. 105 (22) (1996) 9982–9985.
[36] P.E. Blöchl, Projector augmented-wave method, Phys. Rev. B 50 (24) (1994) 17953–17979.
[37] G. Kresse, D. Joubert, From ultrasoft pseudopotentials to the projector augmented-wave method, Phys. Rev. B 59 (3) (1999) 1758.
[38] W. Cai, Dislocation core effects on mobility, Dislocations in Solids, 12 2004, pp. 1–80.
[39] C.R. Weinberger, A.T. Jennings, K. Kang, J.R. Greer, Atomistic simulations and continuum modeling of dislocation nucleation and strength in gold nanowires, J. Mech. Phys. Solids 60 (1) (2012) 84–103.
[40] D. Roundy, M.L. Cohen, Ideal strength of diamond, Si, and Ge, Phys. Rev. B 64 (21) (2001) 212103.
[41] M.I. Eremets, I.A. Trojan, P. Gwaze, J. Huth, R. Boehler, V.D. Blank, The strength of diamond, Appl. Phys. Lett. 87 (14) (2005) 141902.
[42] D. Caillard, J.-L. Martin, Thermally Activated Mechanisms in Crystal Plasticity, Elsevier, 2003.
[43] R.L. Fleischer, W. Hibbard, The Relation Between the Structure and Mechanical Properties of Metals, 261 Her Majesty's Stationary Office, London, 1963.
[44] S. Altmann, K. Lodge, A. Lapiccirella, The stacking-fault energy in diamond, Philos. Mag. A 47 (6) (1983) 827–834.
[45] S.H. Van, P.M. Derlet, A.G. Frøseth, Stacking fault energies and slip in nanocrystalline metals, Nat. Mater. 3 (6) (2004) 399–403.
[46] J. Li, Dislocation nucleation: diffusive origins, Nat. Mater. 14 (7) (2015) 656–657.
[47] J. Godet, P. Hirel, S. Brochard, L. Pizzagalli, Evidence of two plastic regimes controlled by dislocation nucleation in silicon nanostructures, J. Appl. Phys. 105 (2) (2009) 2214.
[48] J. Godet, L. Pizzagalli, S. Brochard, P. Beauchamp, Theoretical study of dislocation nucleation from simple surface defects in semiconductors, Phys. Rev. B 70 (5) (2007) 054109.
[49] C.R. Weinberger, W. Cai, Plasticity of metal nanowires, J. Mater. Chem. 22 (8) (2012) 3277.
[50] J.E. Dorn, J. Mitchell, F. Hauser, Dislocation dynamics, Exp. Mech. 5 (11) (1965) 353–362.
[51] A.L. Ruoff, On the yield strength of diamond, J. Appl. Phys. 50 (5) (1979) 3354.